P-07-26

Extended evaluation of SWIW-tests in KSH02, a method study

Rune Nordqvist, Geosigma AB

March 2007

Svensk Kärnbränslehantering AB
Swedish Nuclear Fuel
and Waste Management Co
Box 5864
SE-102 40 Stockholm Sweden
Tel 08-459 84 00
+46 8 459 84 00
Fax 08-661 57 19
+46 8 661 57 19

ISSN 1651-4416
SKB P-07-26

Extended evaluation of SWIW-tests in KSH02, a method study

Rune Nordqvist, Geosigma AB

March 2007

Keywords: SWIW test, Tracer test, Uranine, Cesium, Tracer test evaluation, Tracer test simulation, Regression analysis.

Abstract

SWIW tests (Single Well Injection Withdrawal) have been carried out in borehole KSH02. Two borehole sections were tested: 422.3–423.3 m and 576.8–579.8 m. A non-sorbing tracer (Uranine) and a sorbing tracer (Cesium) were injected simultaneously in each test. Both of the tests resulted in high-quality data with clearly visible retardation effects for Cesium. Basic evaluation of the tests was carried out using a radial flow and transport model with advection, dispersion and linear equilibrium sorption /Gustafsson and Nordqvist 2005/. A good fit between model and experimental data was obtained except for the tailing parts of the tracer breakthrough curves.

In this report, a simple radial flow and transport model with homogeneous immobile regions was employed to further evaluate experimental data from section 422.3–423.3 m in KSH02. A few generic examples are presented along with examples of best-fit regression analysis of experimental data.

The regression analysis indicates that inclusion of diffusion-type processes may improve the fit between model and data, and explain the tailing, for this test compared with previous evaluation with an advection-dispersion model.

Sammanfattning

SWIW-tester (Single Well Injection Withdrawal) har genomförts i borrhål KSH02. Tester har gjorts i två borrhålssektioner: 422.3–423.3 m samt 576.8–579.8 m. Ett icke-sorberande spårämne (Uranin) och ett sorberande spårämne (Cesium) injicerades samtidigt. Testerna genomfördes utan större komplikationer och experimentdata visade på en tydlig retardationseffekt för Cesium jämfört med Uranin.

En basutvärdering av testerna finns presenterad i en tidigare rapport /Gustafsson och Nordqvist 2005/. Denna utvärdering gjordes med en relativt enkel simuleringsmodell med antagande om radiellt flöde och transport med advektion, dispersion samt linjär jämviktssorption som transportprocesser. Allmänt erhölls bra överensstämmelse mellan modell och experimentdata med undantag av den senare delen av genombrottskurvan för det återpumpade spårämnet.

Denna rapport redogör för en utökad utvärdering av resultaten från den ena av testsektionerna i KSH02, 422.3–423.3 m, där den tidigare utvärderingsmodellen utökats med retention av spårämne i immobila regioner. Rapporten innehåller generiska simuleringsexempel samt anpassning av experimentdata till utvärderingsmodell med hjälp av regressionsanalys.

Resultaten från regressionsanalysen indikerar att antagande av utbyte av spårämne till immobila zoner genom diffusionsprocesser kan bidra till att förbättra överensstämmelsen mellan modell och experimentdata.

Contents

1 Introduction

SWIW (Single Well Injection Withdrawal) tests were carried out in borehole KSH02 during 2004 /Gustafsson and Nordqvist 2005/. Two borehole sections were tested: 422.3–423.3 m and 576.8–579.8 m. A non-sorbing tracer (Uranine) and a sorbing tracer (Cesium) were injected simultaneously in each test. Both of the tests resulted in high-quality data with clearly visible retardation effects for Cesium.

A basic evaluation of the tests was carried out assuming radial flow and transport in a homogeneous formation. The transport processes considered were advection, hydrodynamic dispersion and linear equilibrium sorption. The evaluation resulted in fairly good agreement between the evaluation model and experimental data. However, there were tendencies towards lack of fit at the end of the tracer breakthrough curves. This was especially significant for the test carried out in section 422.3–423.3 m. In this case, the total experimental time was relatively long, providing more contact time for the tracers with the surrounding rock. One possibility is that time-dependent processes such as matrix diffusion or other types of mass exchange with immobile zones may affect experimental results.

The purpose of the work described in this report is to test whether a simple hypothesis of tracer mass exchange with immobile zones may explain some of the discrepancies found in the initial basic evaluation.

2 Background

2.1 Outline of SWIW (Single Well Injection Withdrawal) tests

A SWIW test may consist of all or some of the following phases:

1. Injection of fluid to establish steady state hydraulic conditions.
2. Injection of one or more tracers.
3. Injection of chaser fluid after tracer injection is stopped, possibly also label the chaser fluid with a different tracer.
4. Waiting phase.
5. Recovery phase.

The waiting phase is sometimes also called the shut-in period or resting period.

The tracer breakthrough data that eventually are used for evaluation are obtained from the recovery phase. The injection of chaser fluid has the effect of pushing the tracer out as a "ring" in the formation surrounding the tested section. This is generally a benefit because when the tracer is pumped back both the ascending and descending parts are obtained in the recovery breakthrough curve. During the waiting phase there is no injection or withdrawal of fluid. The purpose of this phase is often to increase the time available for time-dependent transport-processes so that these may be more easily evaluated from the resulting breakthrough curve. A schematic example of a resulting breakthrough curve during a SWIW test is shown in Figure 2-1.

The design of a successful SWIW test requires prior determination of injection and withdrawal flow rates, duration of tracer injection, duration of the various experimental phases, selection of tracers and tracer injection concentrations.

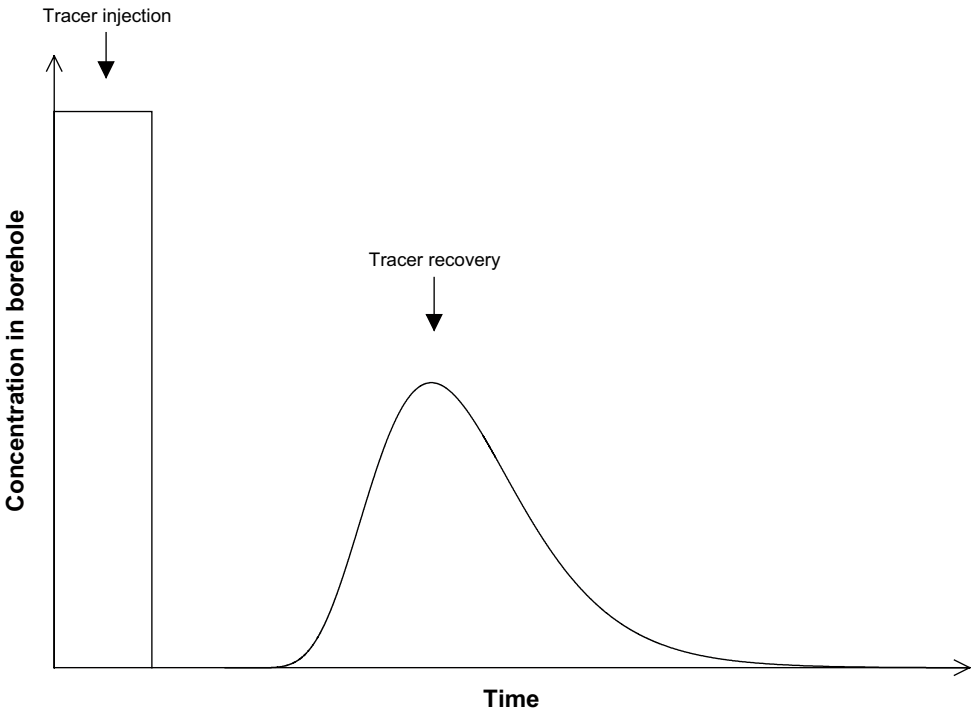

Figure 2-1. *Schematic tracer concentration sequence during a SWIW test /from Andersson 1995/.*

2.2 Previous basic evaluation of SWIW-tests in KSH02

The first basic evaluation of the experimental results in KSH02 was carried out assuming homogeneous conditions and insignificant hydraulic background gradient /Gustafsson and Nordqvist 2005/. Model simulations were made using SUTRA /Voss 1984/. It was assumed that flow and transport occurs within a planar fracture zone of some thickness. The volume available for flow was represented by assigning a porosity value to the assumed zone. Modelled transport processes included advection, dispersion and linear equilibrium sorption.

The sequence of the different injection phases were modelled as accurately as possible based on supporting data for experimental flows and tracer injection concentration. Generally, experimental flows and times may vary from one phase to another, and the flow may also vary within phases.

In the simulation model, tracer injection was simulated as a function accounting for mixing in the borehole section and sorption (for Cesium) on the borehole walls.

Non-linear regression was used to fit the simulation model to experimental data. The estimation strategy was generally to estimate the dispersivity (a_L) and a retardation factor (R), while setting the porosity (i.e. the available volume for flow) to a fixed value. Simultaneous fitting of both tracer breakthrough curves (Uranine and Cesium), and calculation of fitting statistics, was carried out using the approach described in /Nordqvist and Gustafsson 2004/.

The results from the regression analysis, for both of the tested borehole sections, are summarised in Figures 2-2a and 2-2b. These figures indicate a fairly good fit between model and experimental data. However, there is a discrepancy in the tailing part of the Uranine curve in both cases and a similar discrepancy also for Cesium in section 422.3–423.3 m.

The extended evaluation in this report focuses on the latter section, where the tailing discrepancy occurs for both of the tracers. The total experimental time was also longer in this case. The durations of the different experimental phases are presented in Table 2-1.

Table 2-1. Durations (hours) and fluid flows (L/h) during various experimental phases for section 422.3–423.3 m /from Gustafsson and Nordqvist 2005/.

Phase	Start (h)	Stop (h)	Volume (L)	Average flow (L/h)	Cumulative injected volume (L)
Tracer injection	0	0.95	14.25	15.0	14.25
Chaser injection 1	0.95	13.12	163.1	13.4	177.35
Waiting phase 1	13.12	15.17	0	0	177.35
Chaser injection 2	15.17	63.50	26.6[1]	0.55[1]	203.95
Waiting phase 2	63.50	65.20	0	0	203.95
Recovery	65.20	182.98	1,767	15.0	–

[1)] These values are calculated using an estimate of transmissivity based on differential flow logging and hydraulic injection tests.

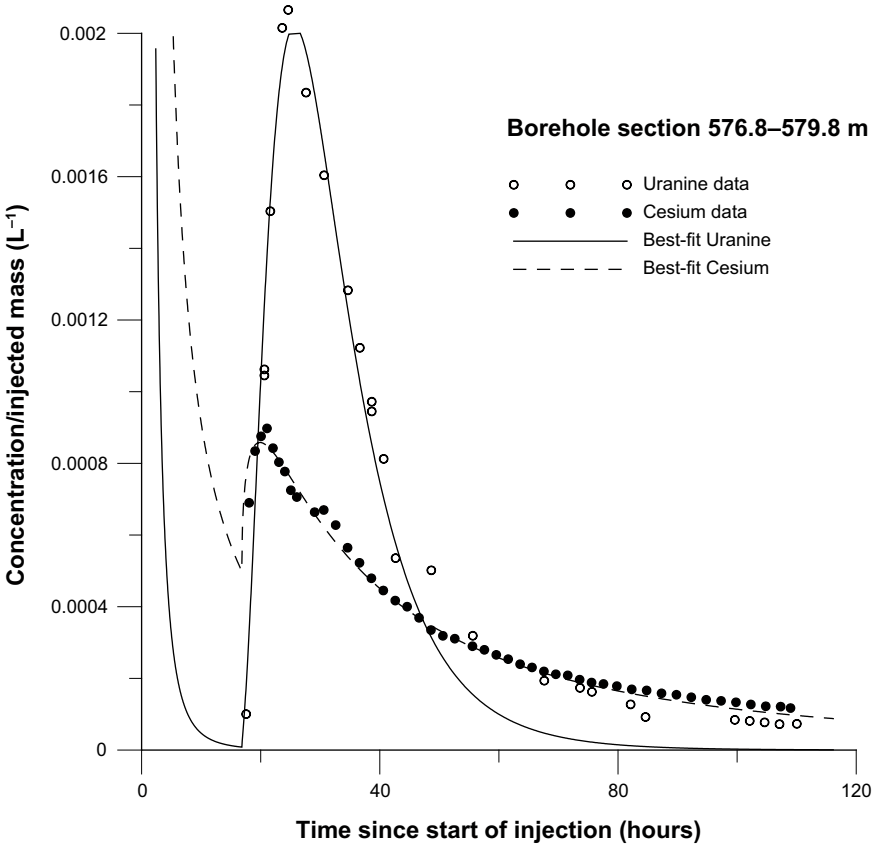

Figure 2-2a. *Best-fit basic evaluation of the SWIW test in section 576.8–579.9 m.*

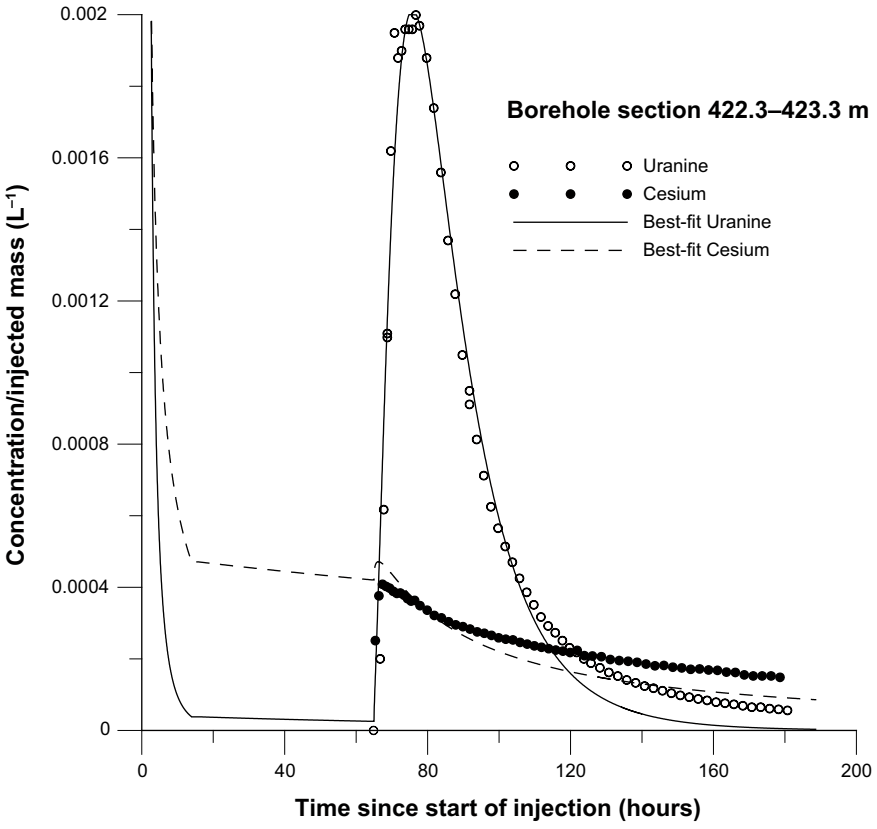

Figure 2-2b. *Best-fit basic evaluation of the SWIW test in section 422.3–423.3 m.*

3 Simulation approach

The simulations including matrix diffusion are carried out assuming a vertical section with radial symmetry. The simulated geometry approximately corresponds to a dual-porosity approach based on the assumption of parallel fractures and is schematically illustrated in Figure 3-1. A similar simulation approach was used by /Lessoff and Konikow 1997/.

The solute transport is simulated with the standard advection-dispersion model in two dimensions. The dispersion coefficients in the longitudinal (D_L) and transverse (D_T) directions, respectively, are commonly expressed by:

$$D_L = a_L\, v + D_m \qquad (3\text{-}1)$$

$$D_T = a_T\, v + D_m \qquad (3\text{-}2)$$

where a_L and a_T are the longitudinal and transverse dispersivities, respectively, v is the magnitude of the water velocity and D_m is the diffusion coefficient. In the radial cross-section, significant flow only takes place in the x-direction in the thin layer that represents the fracture and here the advective terms dominate. However, the transverse dispersivity has very little effect in this case, because all simulations are carried out in a cross section with radial symmetry.

In the stagnant matrix the diffusion term dominates.

The layout in Figure 3-1 represents a single plane-parallel fracture with a width of 0.0002 m (half width = 0.0001 m) having a porosity of 1.0. The stagnant matrix (simulated with a very low value of hydraulic conductivity) extends, on both sides of the fracture, to a distance of 0.2 m away from the centre of the fracture. The model extends 40 m in the radial direction, which is intended to be well beyond the distances that solute may travel during the fluid injection phases. A porosity value is assigned to the stagnant matrix as well as a diffusivity value. The latter is pore diffusivity, which is less than diffusivity in water due to tortuosity and constrictivity effects.

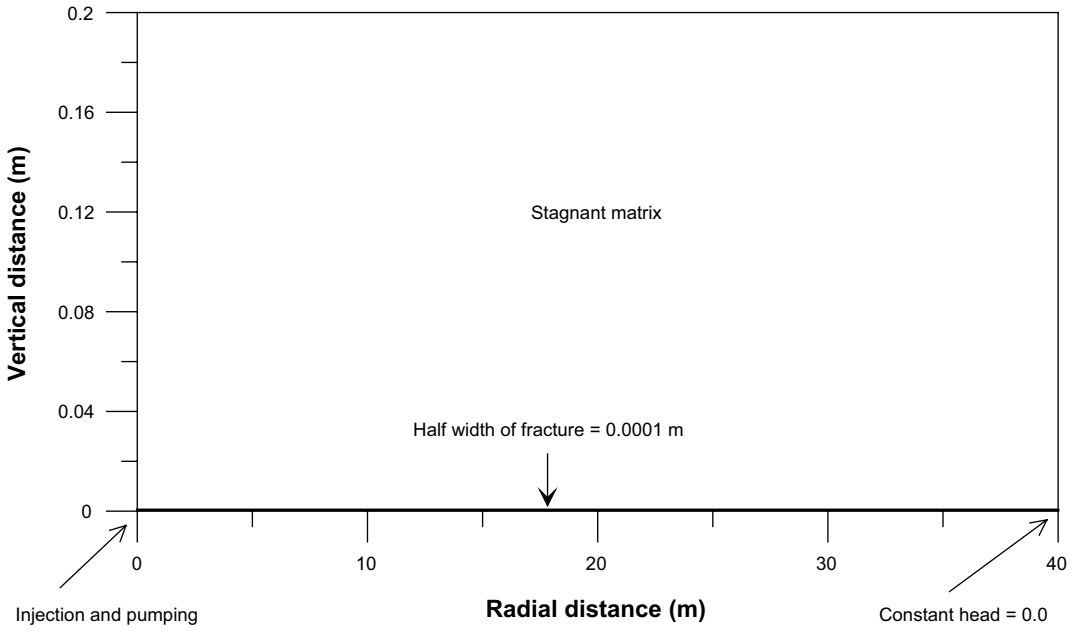

Figure 3-1. *Layout for simulation of SWIW test in a fracture with matrix diffusion.*

Sorption in the matrix is simulated assuming linear equilibrium sorption (K_d-sorption). One-dimensional transport of a sorbing tracer by diffusion may be described by:

$$\frac{\partial C_m}{\partial t} = \frac{D_p}{R_m}\frac{\partial^2 C_m}{\partial z^2} \tag{3-3}$$

where C_m is solute concentration in the matrix [M/L^3], D_p is the pore diffusivity [L^2/T]. The matrix retardation factor, R_m, is given by:

$$R_m = 1 + \frac{\rho_s (1 - p_{matrix})}{p_{matrix}} K_d \tag{3-4}$$

where ρ_s is the density of the solid [M/L^3], p_{matrix} is the matrix porosity [–] and K_d is the distribution coefficient for linear equilibrium sorption [L^3/M].

In addition to the simulation model described above, a variant was considered where the immobile part of the simulation domain was divided into two parts. Closest to the flowing fracture, a thin layer was introduced where the porosity may be assigned a different value than the rest of the matrix. This layer may then represent relatively porous coating material or simply be used to represent non-flowing parts of the fracture.

Non-linear regression was used to fit the simulation model to experimental data. Simultaneous fitting of both tracer breakthrough curves (Uranine and Cesium), and calculation of fitting statistics, was carried out using the same approach as in the previous evaluation of this test /Gustafsson and Nordqvist 2005/.

In the next section, a few generic simulation results are shown in order to illustrate the combined effects of matrix diffusion and matrix sorption on SWIW experiments. In /Nordqvist and Gustafsson 2002/, similar simulations were presented but without consideration of these processes in combination.

4 Results

4.1 Generic simulations of SWIW tests with matrix diffusion

In this section, a few generic examples are presented in order to illustrate the effects of combined matrix sorption and diffusion on SWIW experiments. The simulation model is the one described in the preceding section. These simulations were run with the following durations of the various experimental phases:

- Tracer injection duration: 1 hour
- Chaser injection duration: 12 hours
- Waiting phase duration: 50 hours

These settings are similar to the experimental ones for section 422.3–423.3 m, except that instead of the waiting phase there was a period with a small outflow into the formation due to open borehole conditions.

Examples of tracer recovery curves for different pore diffusivity (D_p) values, but without sorption, are shown in Figure 4-1. The matrix porosity is set to 0.01, a relatively high value, in order to obtain clearly visible simulation effects. Lower porosity values should give similar results but with smaller diffusion effects. The longitudinal dispersivity is set to a fairly small value, 0.25 m. The effect of matrix diffusion on the recovery curves is that peaks are lowered and the tail is somewhat more elongated. There is also a slightly earlier first arrival. However, despite the relatively high porosity values, the effects on the breakthrough curve are not dramatic in the absence of sorption.

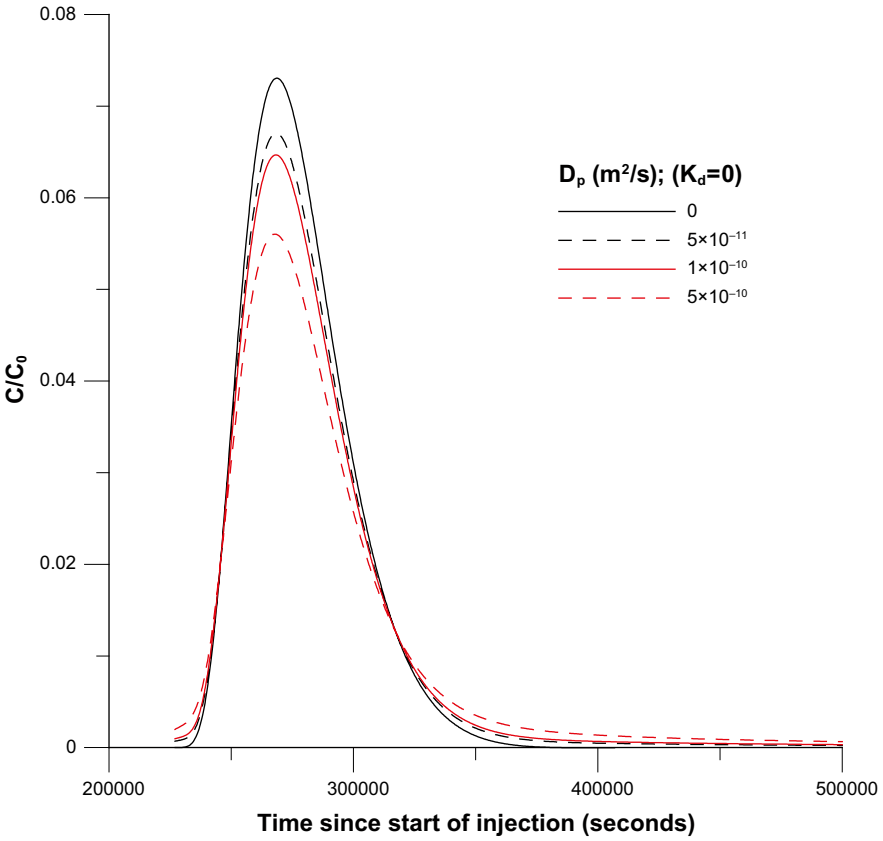

Figure 4-1. *Effects of pore diffusivity on tracer recovery (no sorption).*

The process of diffusion into the matrix during a SWIW experiment, as simulated with this particular model, is illustrated in Figure 4-2, which shows several tracer profiles perpendicular from the flowing fracture into the stagnant matrix for the case of $D_p = 10^{-10}$ m^2/s and a matrix porosity of 0.01. In the simulation shown in Figure 4-2, the tracer has started to diffuse into the matrix (to about 5 mm) already during the chaser injection phase. During the waiting phase, the migration into the matrix continues, resulting in a slight decrease in the concentration in the fracture. During recovery pumping, the tracer in the fracture is pumped back to the test section and the tracer that has entered the matrix begins to diffuse back into the flowing fracture but also continues to migrate further away from the fracture.

If sorption is added to the simulations, significantly more visible effects on the breakthrough curves are obtained. A few examples of the combined effect of sorption and diffusion are shown in Figure 4-3. Figure 4-3 shows tracer recovery curves for several values of the sorption coefficient (K_d). The pore diffusivity is set to a value of 10^{-10} m^2/s.

A general impression from the generic examples is that it may be possible that diffusion processes can have some effect on breakthrough curves under these experimental conditions. It also seems possible that strong sorption in the matrix may give effects similar to what is observed in the experimental data (Figure 2-2b).

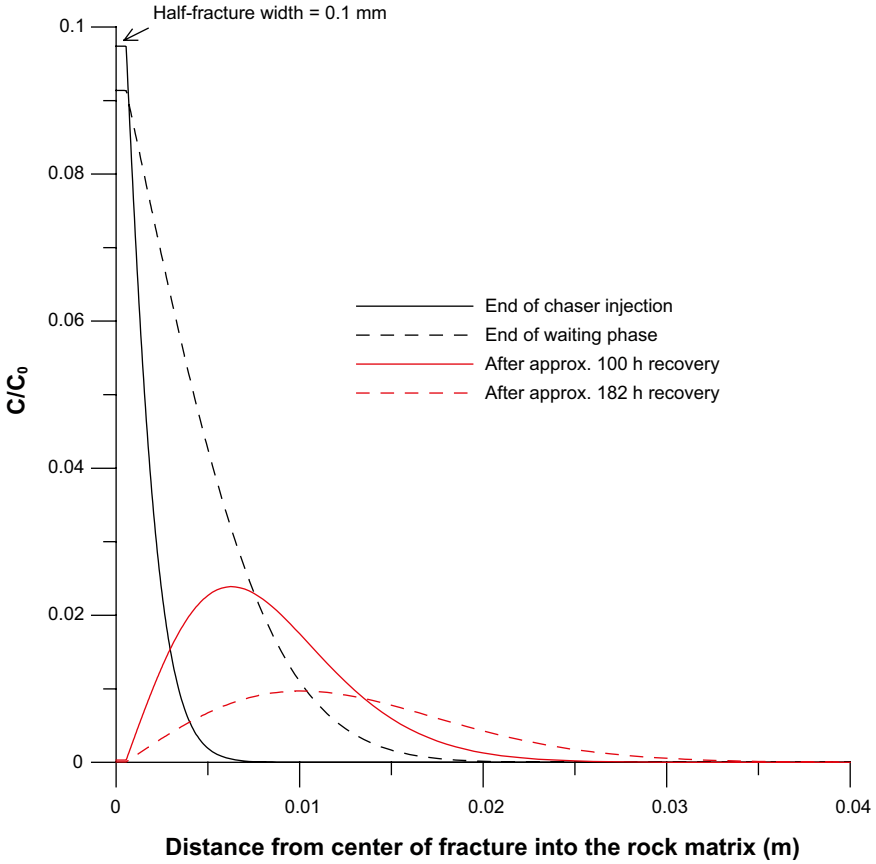

Figure 4-2. *Illustration of a matrix concentration profile from the centre of the fracture into the rock matrix at different stages of a SWIW experiment. The profile shown is located at a radial fracture distance where C/C_0 (C_0 is the injection concentration) in the flowing fracture is at a maximum at the end of the chaser injection phase.*

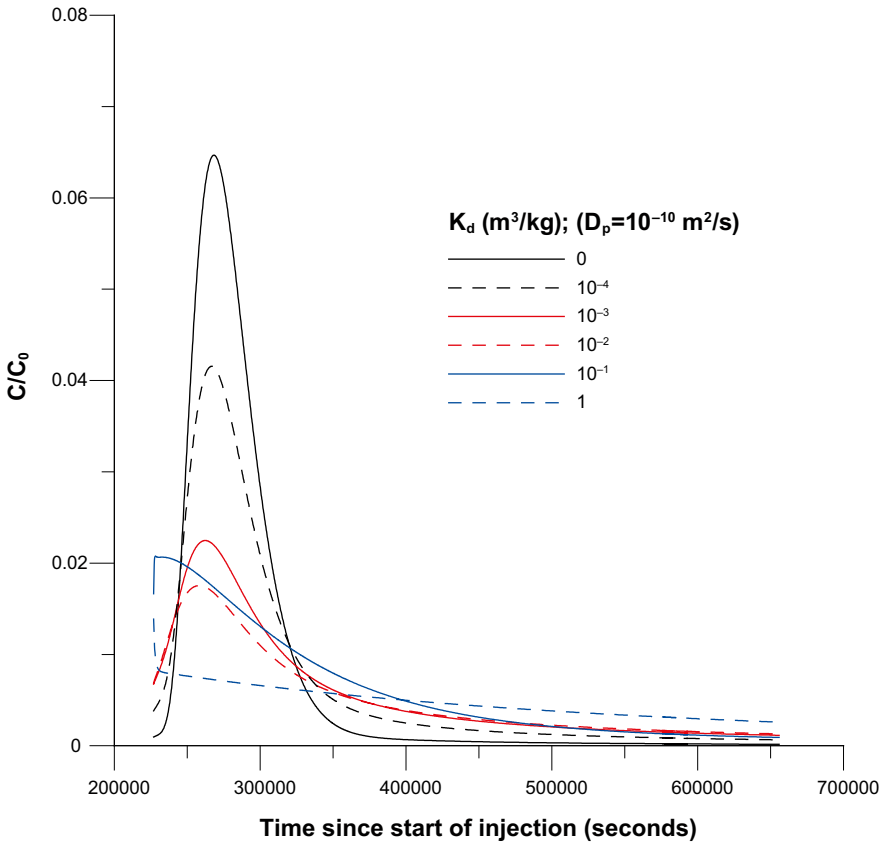

Figure 4-3. *Illustration of the combined effect of matrix diffusion and sorption.*

4.2 Evaluation of KSH02 tests with sorption and matrix diffusion

Using the basic radial model with matrix diffusion outlined in Chapter 3, parameter estimation with non-linear regression was carried out on the experimental SWIW results from section 422.3–423.3 m in KSH02. The parameter estimation strategy in such a case may be devised in many different ways regarding choice of which parameters should be estimated and which parameters should be held fixed. A summary of the main assumptions for the parameter estimation study is as follows:

- Fixed values were assumed for the pore diffusivity (D_p). The value of D_p for Uranine was set to 1×10^{-10} m^2/s and five times higher for Cesium. These assumptions are rather arbitrary and only intended to be approximate, but nevertheless somewhat lower than corresponding values in water. /Ohlsson and Neretnieks 1995/, for example, reported diffusivities in water for Uranine and Cesium, respectively, of 4.5×10^{-10} and 2.4×10^{-9} m^2/s.
- The aperture of the flowing fracture is held fixed at a value of 2×10^{-4} m. This value is also somewhat arbitrary, although it is chosen to be approximately consistent with an interpreted transmissivity value for the section and the cubic law.
- Matrix porosity (p_{matrix}) is an estimation parameter.
- Sorption coefficient (K_d) is an estimation parameter.
- Longitudinal dispersivity (a_L) is an estimation parameter in some of the cases.

A proportionality factor is also included as an estimation parameter. This factor accounts for any proportional uncertainty in injection concentrations or possible experimental tracer losses, for example. Note that both of the tracer curves are estimated simultaneously using the same proportionality factor.

In addition to the basic model outlined above, a variant is performed where the immobile region (matrix) is divided into two parts (layers). A thin layer (rim zone) adjacent to the flowing fracture is allowed to have a different porosity value than the rest of the matrix. This layer is thought to approximately represent, for example, more porous fault gouge material and/or simply immobile volumes of water.

The estimation examples with the basic matrix diffusion model are presented in Section 4.2.1 and the cases with the rim zone model in Section 4.2.2.

4.2.1 Model fitting with the basic matrix diffusion model

Model fit of Uranine data alone

Figure 4-4 shows a model fit of Uranine alone to the experimental data with the basic model outlined in Chapter 3. Thus, Cesium is not fitted in this example. Model fitting on Uranine alone provides a first impression of the possibility of explaining the tailing by consideration of a diffusion process. The model fit is in this case relatively good for the entire recovery curve. Estimated parameter values are: $p_{matrix} = 1.5\times10^{-2}$ and $a_L = 0.99$ m. The model fit is good but requires a relatively high best-fit value of the matrix porosity. However, despite the high value for matrix porosity, it appears plausible that diffusion is one possible explanation for the tailing in the Uranine breakthrough curve.

Model fit of Cesium data with fixed matrix porosity and dispersivity

This example shows fitting of Cesium data alone, using fixed values of matrix porosity and longitudinal dispersivity obtained from the preceding example. Thus, this may be regarded as a step-wise procedure where the non-sorbing tracer is used to determine the matrix porosity and dispersivity in a first step, followed by a second step where the parameters estimated in the first step are held fixed and only the sorption coefficient is estimated.

The model fit is shown in Figure 4-5. The fit to the Uranine curve is identical to the preceding case because all parameters affecting this curve are held fixed. The fit to the Cesium curve appears to be relatively good, except that the simulated curve is slightly lower than the experimental one. The sorption coefficient (K_d) is estimated to 1.5 m^3/kg.

Clearly visible effects of back-diffusion in the model simulations are seen in Figure 4-5 during the waiting phases. The simulated effects of back-diffusion are not completely consistent with the beginning of the recovery breakthrough curve for Cs. However, detailed model comparison close to transitions from one experimental phase to another should be regarded only as approximate. The simulation model calculates concentrations at nodes placed at the borehole wall and this is likely not entirely representative for the concentration in the borehole section (i.e. what enters the sampling tubing in the section) when pumping conditions change.

Simultaneous fit of Uranine and Cesium

This example show simultaneous fitting of Uranine and Cesium data, with the matrix porosity, longitudinal dispersivity and the sorption coefficient as estimation parameters. This case is equivalent to the combination of the two preceding examples, except that all parameters are estimated at once instead of in a step-wise procedure. It may be argued that simultaneous fitting should be better because it allows more flexibility in finding parameter values that provide a good fit to both data sets.

The resulting fit is shown in Figure 4-6. The fit is fairly good, except that the tail of the Uranine curve is somewhat over-estimated. The resulting parameter values are: matrix porosity = 2.5×10^{-2}, dispersivity = 0.63 m and the sorption coefficient = 3.0 m^3/kg.

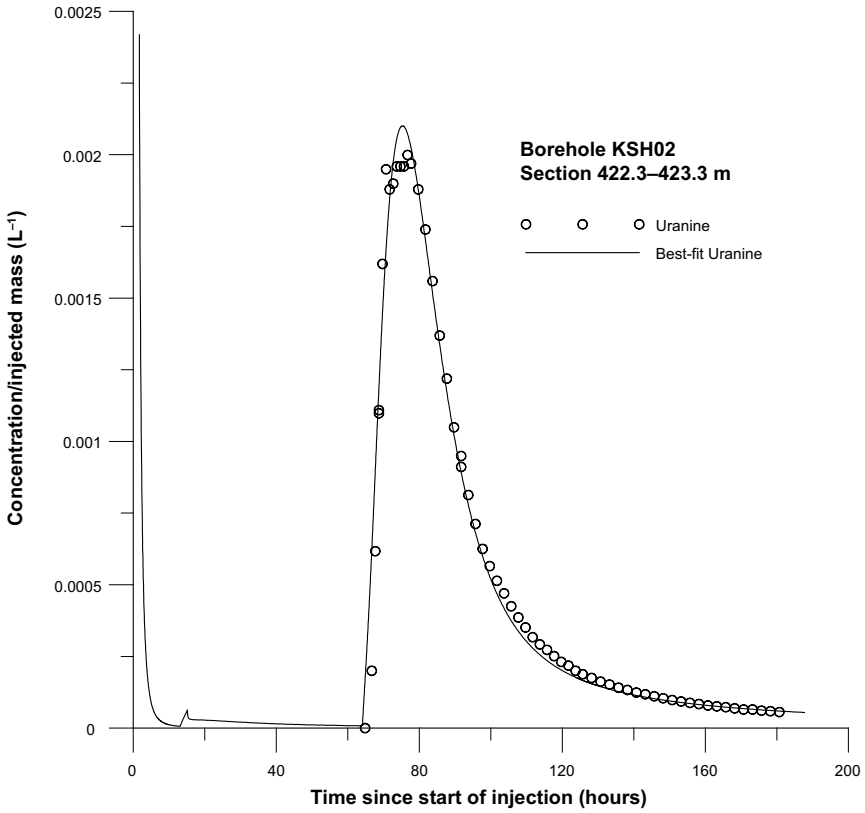

Figure 4-4. *Model fit of Uranine data alone. Parameter estimates are:* $p_{matrix} = 1.5 \times 10^{-2}$ *and* $a_L = 0.99$ *m.*

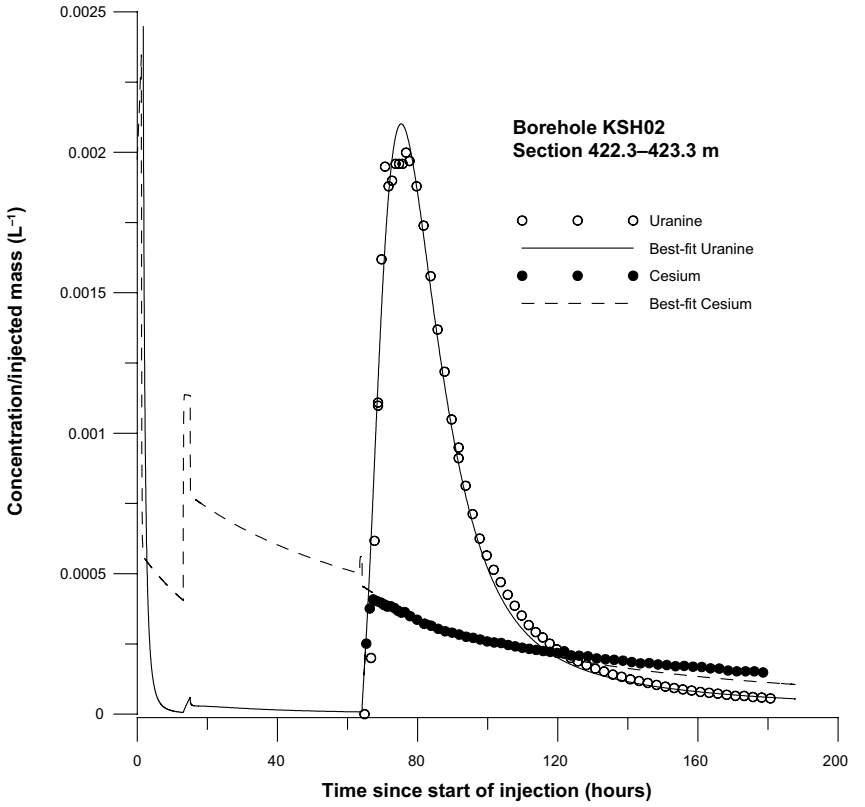

Figure 4-5. *Model fit of Cesium data alone (the Uranine fit is identical to the preceding case). The estimated value for the sorption coefficient* (K_d) *is 1.5* m^3/kg.

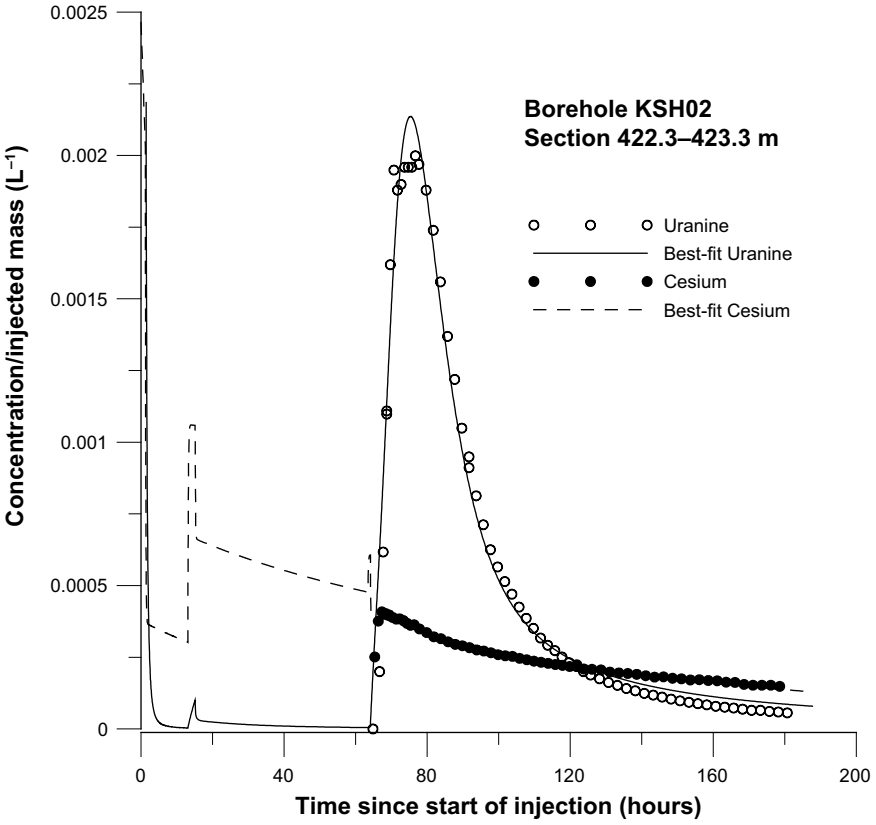

Figure 4-6. *Simultaneous fit of Uranine and Cesium data. Estimated values are:* $p_{matrix} = 2.5\times10^{-2}$, $a_L = 0.63$ *m,* $K_d = 3.0$ m^3/kg.

Simultaneous fit of Uranine and Cesium with minimum dispersion

This case is identical to the preceding one except that the value for longitudinal dispersivity is set to a fixed value. The intention of this estimation scenario is to see to what extent diffusion and sorption in the matrix alone can explain the experimental results. With consideration taken to the element discretisation of the simulation model, a minimum value of dispersivity is set to 0.25 m.

With the longitudinal dispersivity set to a fixed low value, the model fit (Figure 4-7) is somewhat worse compared with preceding cases. Estimated parameter values are: matrix porosity (p_{matrix}) = 3.6×10^{-2}, sorption coefficient (K_d) = 6.3 m^3/kg.

4.2.2 Model fitting with basic model with rim zone

Simultaneous fit of Uranine and Cesium

As an extension to the basic matrix diffusion model, a slightly more complex model with the matrix divided into two layers was applied to evaluate the experimental data. The layer closest to the open fracture is assumed to be relatively thin (set to a value of 0.58 mm) and thought to represent some kind of rim zone that might be expected to have higher porosity than the matrix. An alternative interpretation is that this layer might represent a volume with immobile water available for diffusive exchange with the flowing part of the fracture.

Estimated parameter values are in this case: rim porosity = 0.37, matrix porosity = 4.4×10^{-2}, longitudinal dispersivity = 0.44 m, sorption coefficient (K_d) = 0.16 m^3/kg. Note that the same K_d-value is used for both of the non-flowing layers, which may not be realistic. The effective

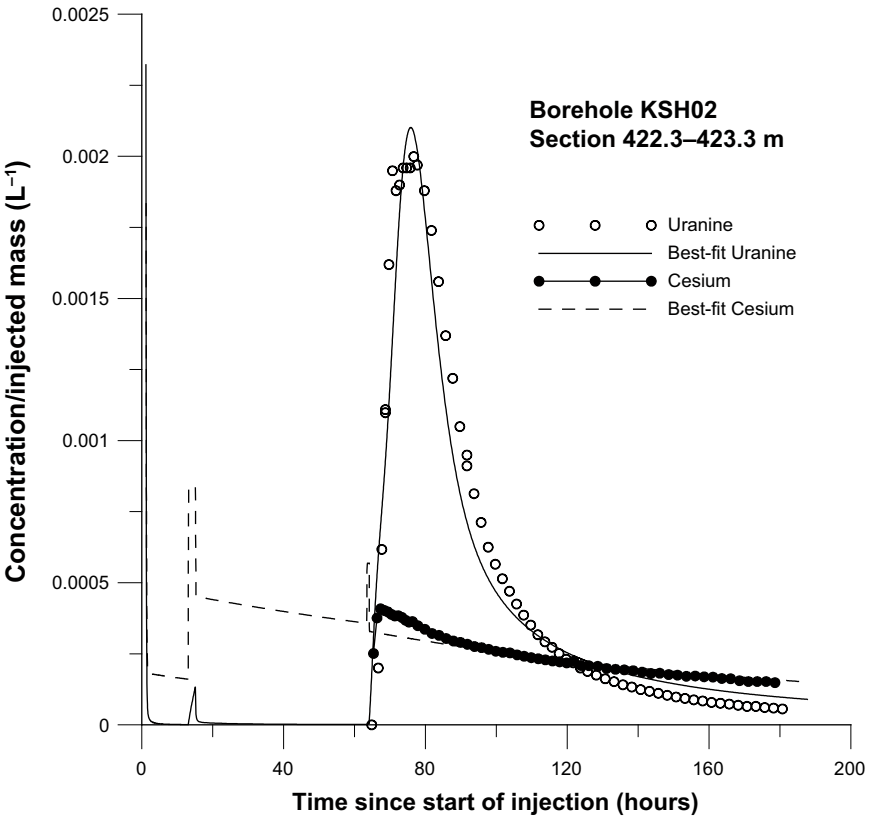

Figure 4-7. *Simultaneous fit of Uranine and Cesium data with the longitudinal dispersivity set to a fixed value of 0.25 m. Estimated parameter values are:* $p_{matrix} = 3.6\times10^{-2}$, $K_d = 6.3$ m^3/kg.

retardation effect in the two non-flowing layers is thus differentiated by the estimation of different porosity values (i.e. equation 3-4). However, the intention of this simulation case is to obtain an overall impression whether a dual-porosity non-flowing part might significantly increase the possibilities to explain the experimental data.

The model fit in this case (Figure 4-8) may be considered the best one of all of the examples presented above, although this may not be surprising since another fitting parameter is added. However, the estimated parameter values are consistent with the prior assumption that the rim zone should represent some volume with relatively high porosity.

The estimated K_d-value may be approximately translated to a surface sorption coefficient, K_A, by considering the total sorption capacity per unit surface of the rim zone:

$$K_A \approx K_d \, b_{rim} \, \rho_s \, (1-p_{matrix}) \qquad (4\text{-}1)$$

where b_{rim} is the thickness of the rim zone [L]. This is only a rough approximation because diffusion in the rim zone is neglected. The fracture retardation factor, R_A, for a smooth parallel fracture is:

$$R_A = 1 + \frac{2}{b} K_A \qquad (4\text{-}2)$$

where b is the fracture aperture [L].

This gives an approximate value of K_A of 0.15 m, which results in a retardation factor for the flowing fracture of about 1,500. This is a very high fracture retardation factor, but nevertheless on the same order as previous estimates (about 1,000) from the basic evaluation with an advection-dispersion model /Gustafsson and Nordqvist 2005/.

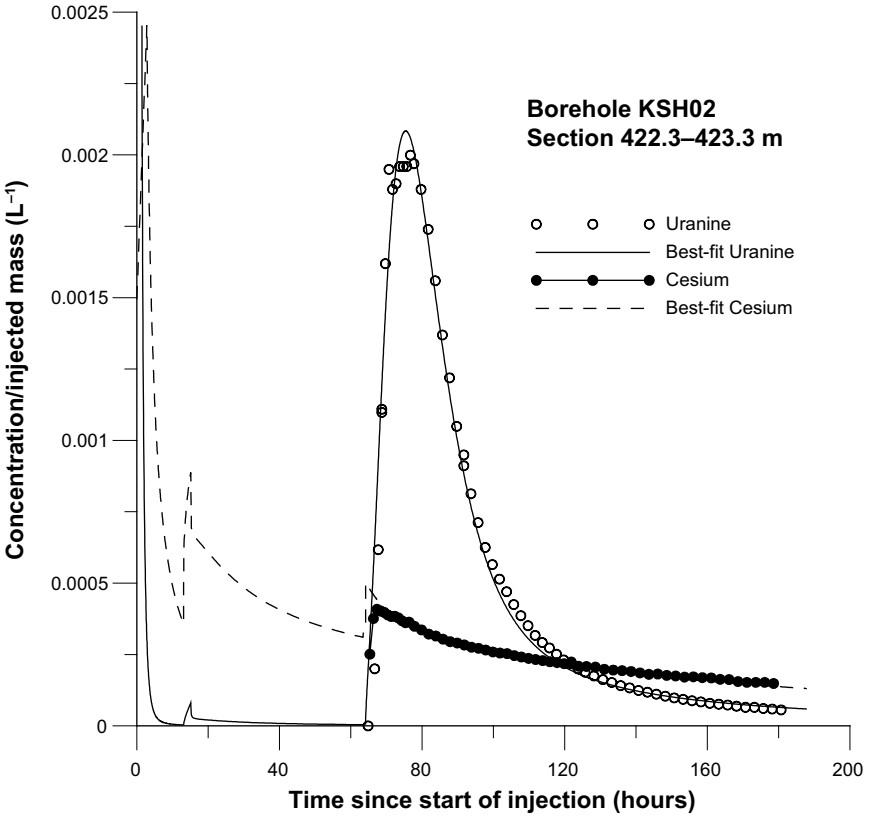

Figure 4-8. *Simultaneous fitting of Uranine and Cesium data with the rim zone model. Estimated parameter values are:* $p_{rim} = 0.37$, $p_{matrix} = 4.4\times10^{-2}$, $a_L = 0.44$ m, $K_d = 0.16$ m^3/kg.

It may be added that the theoretical advective radial travel distance for a non-sorbing tracer is about 16.5 m at the end of the chaser injection phase, for the conditions listed in Table 2-1 and other simulation settings. The corresponding theoretical travel radial distance for a tracer with a fracture retardation factor of 1,500 is then only about 0.4 m.

Simultaneous fit of Uranine and Cesium with minimum dispersion

As for the basic matrix diffusion model, a case was run with a fixed minimum value of the longitudinal dispersivity (0.25 m). The model fit (Figure 4-9) is good and very similar to the fit in the preceding case. Estimated values are: rim porosity = 0.57, matrix porosity = 7.2×10^{-2}, sorption coefficient (K_d) = 0.43 m^3/kg. The latter value is almost three times higher than in the preceding case and may be translated to a retardation factor in the flowing fracture to about 2,900.

4.2.3 Summary of the parameter estimation analysis

A summary of the various parameter estimation cases is presented in Table 4-1. The most obvious difference between the basic matrix diffusion model and the model with the added rim zone is that the estimated K_d values differ considerably. The model with the rim zone has about an order of magnitude lower K_d values, combined with a rim zone of high porosity values.

A comparison of the model fits in the preceding sections indicates that the model with the added rim zone results in a better fit with experimental data. The basic model also requires large K_d-values and large matrix porosity values in order to fit data (although the rim zone model also gives high matrix porosity values). Based on this, it may be argued that the results suggest that sorption of Cesium primarily occurs close to the flowing fracture and may thus be regarded as fracture surface sorption.

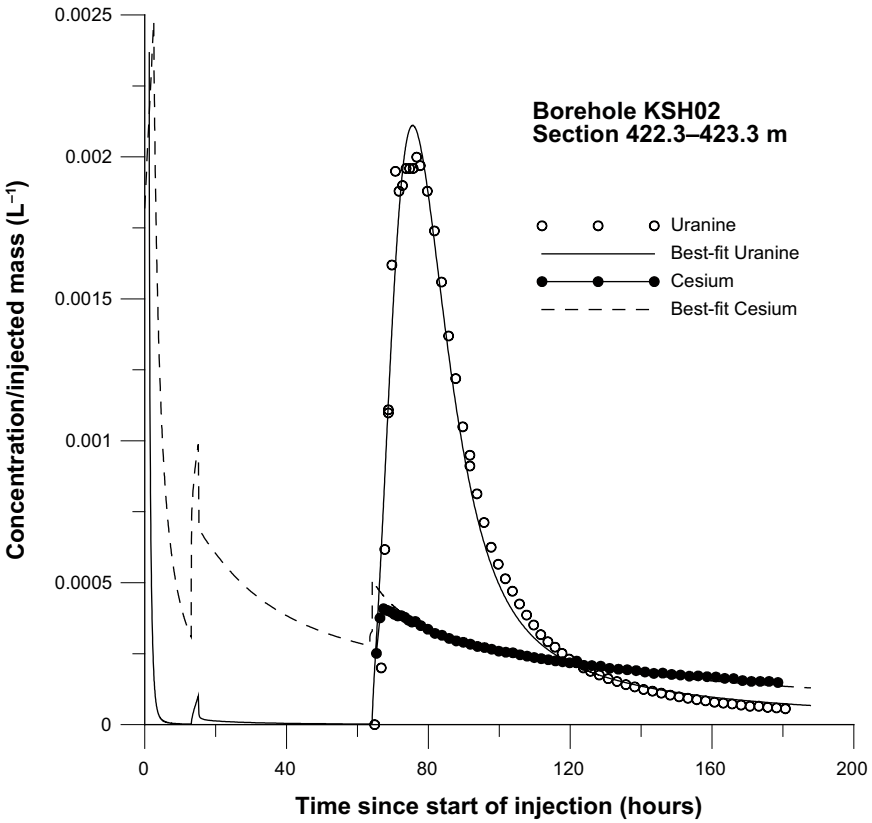

Figure 4-9. *Simultaneous fit of Uranine and Cesium data with the longitudinal dispersivity set to a fixed value of 0.25 m. Estimated parameter values are:* $p_{rim} = 0.57$, $p_{matrix} = 7.2\times10^{-2}$, $K_d = 0.43$ m^3/kg.

Table 4-1. Summary of parameter estimation results.

Case	Fixed parameters	Estimated parameters			
		p_{matrix}	p_{rim}	a_L (m)	K_d (m^3/kg)
Basic model Ur only		1.5×10^{-2}	–	0.99	–
Basic model Cs only	p_{matrix} (1.5×10^{-2})* a_L (0.99 m)*	–	–	–	1.5
Basic model Ur+Cs		2.5×10^{-2}	–	0.63	3.0
Basic model Ur+Cs	a_L (0.25 m)	3.6×10^{-2}	–	–	6.3
Rim model Ur+Cs		4.4×10^{-2}	0.37	0.44	0.15
Rim model Ur+Cs	a_L (0.25 m)	7.2×10^{-2}	0.57	–	0.43

* Parameter values for the fixed parameters obtained from the case with Uranine only.

4.2.4 Comments on tracer recovery

Because concentration values at the end of the experimental tracer breakthrough curves are clearly above background values, the ultimate tracer recovery can not be estimated using experimental data alone. As reported in /Gustafsson and Nordqvist 2005/, recovered tracer mass at the end of the experimental curves amounts to about 86% for Uranine and 41% for Cesium.

Final tracer recovery values, i.e. that would have resulted if pumping had been carried out until tracer background values were obtained, can not be estimated without extrapolation of the experimental curves. Such extrapolation is difficult because the tailing parts of the curves might be extensive.

One method for extrapolation of the experimental curves is to use a well-fitting model simulation, which has the obvious appeal of employing some plausible physical process in the extrapolation method. For some of the best-fitting cases above, calculated tracer recovery values based on the fitted simulation model results indicate more or less full recovery for Uranine and possibly also for Cesium (at least 80%). However, any estimates of final recovery values by extrapolation of the experimental curves should be considered very uncertain.

4.3 Generic simulations with multiple fractures

As a complement to the generic simulations in a radial symmetry with matrix diffusion, a few generic simulations were made with an alternative model approach without matrix diffusion, but allowing for multiple fractures (or transport paths) with different advective properties. Consideration of such a model may seem natural because it is entirely conceivable that tracers do not spread evenly in the diverging-converging flow field during a SWIW experiment. In cross-hole tracer tests, there are often indications of multiple transport paths.

One question is then whether allowing for multiple transport paths may provide an alternative explanation for the tailing observed in the SWIW tests in KSH02, as well as in other SWIW tests performed so far within the site investigation programme, see for example /Gustafsson et al. 2005/.

SWIW tests assuming multiple flow paths require consideration of how to distribute flow properties (i.e. transmissivity) amongst the different paths, because mixing in the borehole will depend on the flow rate from each path. Herein it is assumed, as in a study by /Becker and Shapiro 2003/, that the transmissivity, T, of each flow path is related to the aperture, b, by the so called cubic law:

$$T = \frac{\rho g}{12\mu} b^3 \qquad (4\text{-}3)$$

where ρ is the water density [M/L^3], μ is the dynamic viscosity [$ML^{-1}T^{-1}$] and g is the gravitational acceleration [L/T^2].

Simulations are made in fractures assuming radial symmetry. Thus, this simulation example is limited to sets of transport paths with a flow dimension of 2. It is assumed that one may either see this as a combination of different individual fracture planes intersecting the borehole section, but alternatively as a combination of flow paths (with a flow dimension of 2) within a single fracture.

The following experimental time settings are used:

- Tracer injection: 1 hour
- Chaser injection: 12 hours

The injection, chaser and pumping flow (e.g. the total flow in the borehole section) is assumed to be 15 l/h (4.17×10^{-6} m^3/s) and that the transmissivity for the whole section is 10^{-6} m^2/s.

Two main cases are illustrated here:

1. All paths have the same dispersivity, set to 0.25 m (intended to be a low value).
2. Paths may have different dispersivity.

Tracer transport in the individual transport paths were simulated for a range of arbitrarily selected flow rates, the flow rates being different fractions of the total flow rate. The aperture of each fracture was determined from equation 4-1, by assuming that the transmissivity of the individual facture is proportional to the flow rate. For example, if a fracture is assigned a flow that is 1/10 of the total flow rate, it is assumed that the transmissivity of the individual fracture is 1/10 of the total transmissivity.

Having simulated a range of fractures with different flow rates, fractures were arbitrarily combined in order to obtain compound breakthrough curves resulting from multiple fractures in a borehole section.

All of the simulated breakthrough curves for individual fractures for the case of equal dispersivity are shown in Figure 4-10. Ten fractures are simulated, ranging from 0.1, and in step of 0.1, to 1.0 of the total flow rate.

Figure 4-10 shows that there is more tailing in curves for fractures with lower flow rates and indicates that combinations of fractures may give more elongated tails than a single fracture. However, there is also a corresponding elongation of the ascending part of those curves. This is generally not observed in the ascending parts of the experimental SWIW data.

An example of arbitrarily selected combined curves is shown if Figure 4-11.

Figure 4-11 indicates that for any significant tailing to occur, a number of smaller fractures are required. However, in such cases the ascending part of the combined curve is also elongated.

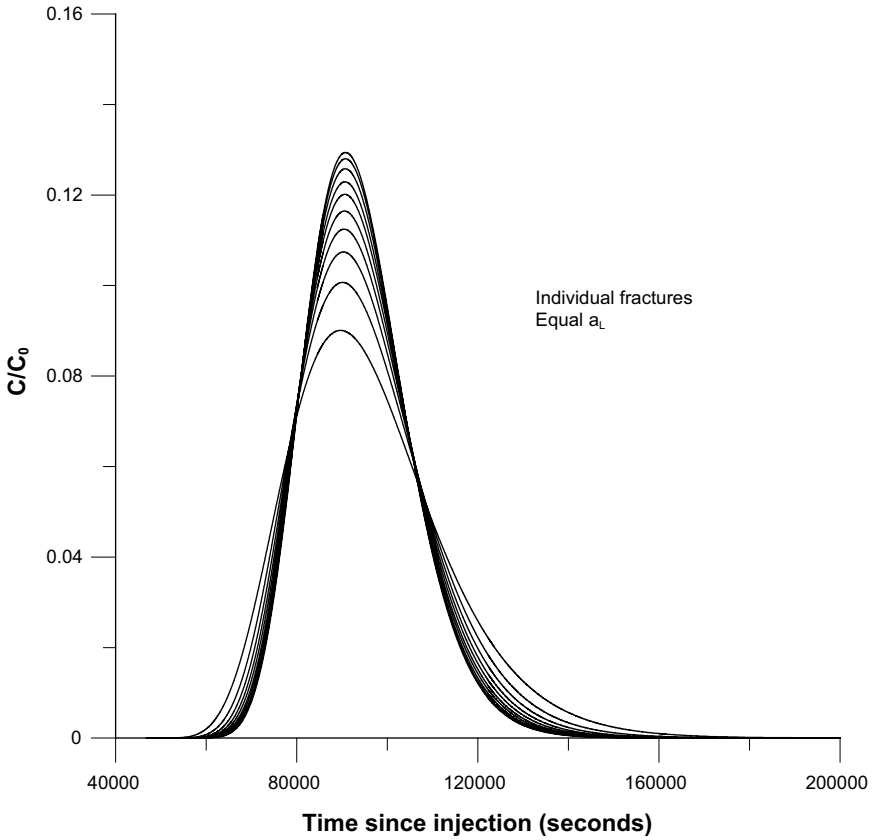

Figure 4-10. *Breakthrough curves for the simulated individual fractures for the case with equal dispersivity. Flow rates range from 0.1 to 1.0 of the total flow rate.*

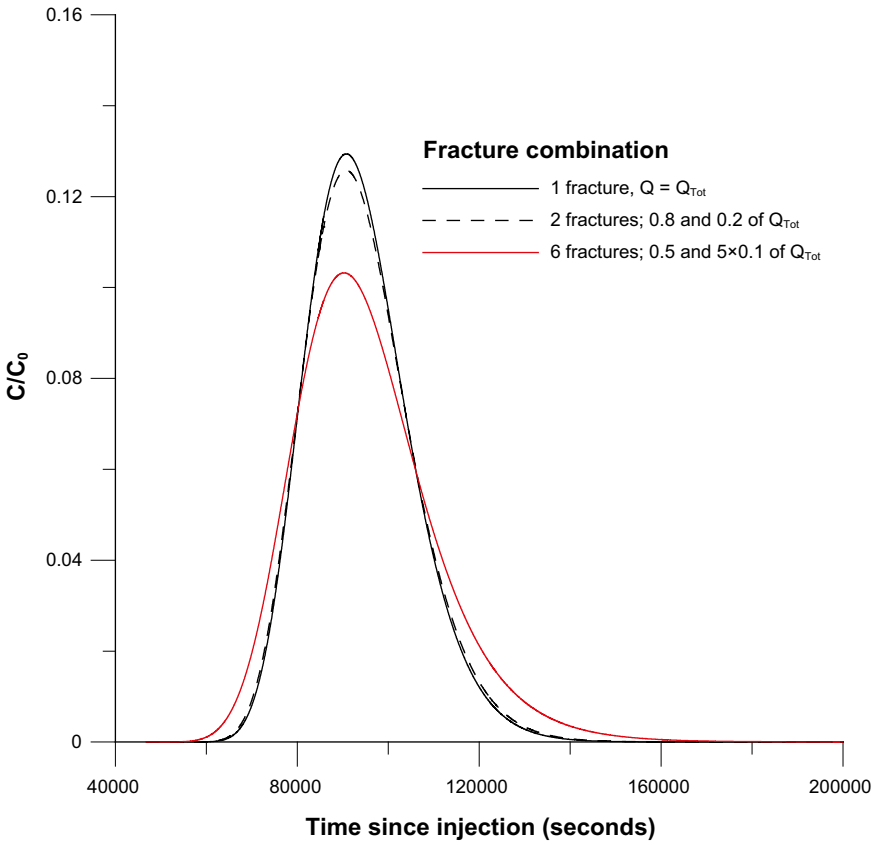

Figure 4-11. *Examples of SWIW breakthrough curves for combinations of fractures with equal dispersivity.*

In the example where individual fractures are allowed to have different dispersivity values, the dispersivity is assigned arbitrarily for some of the fractures according to:

$Q = 0.1\ Q_{Tot}$ $a_L = 1.5$ m

$Q = 0.2\ Q_{Tot}$ $a_L = 1.0$ m

$Q = 0.5\ Q_{Tot}$ $a_L = 0.5$ m

Note that the this assignment of dispersivity values is arbitrary, except that when tracer cross-hole tests are interpreted with multi-paths models, the smaller paths are often associated with higher dispersivity.

Examples of combined curves for the case of unequal dispersion are shown in Figure 4-12.

As fully expected, the combinations of individual fractures in Figure 4-12 show a more pronounced tailing than the example with equal dispersivity. However, also in this case there is a corresponding elongation of the ascending part.

An overall visual impression of the simulations in this section is that none of the results appear to resemble the shapes of the experimental breakthrough curves (Figures 2-2a and 2-2b). The experimental curves have a sharp ascending part, as well as the beginning of the descending part flowed by an elongated tail.

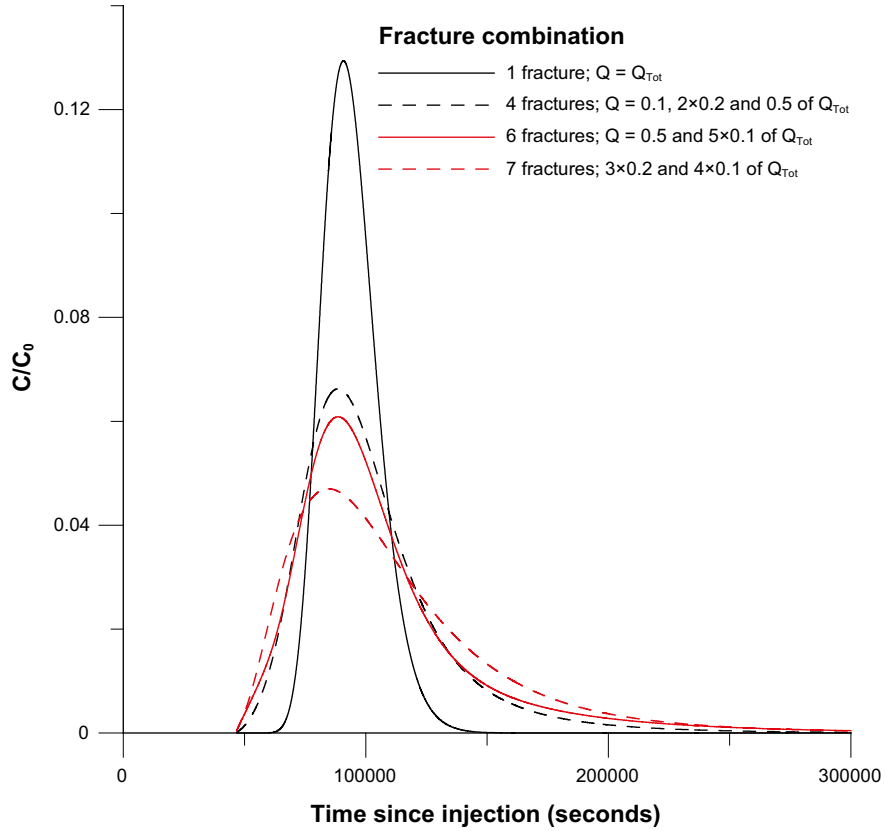

Figure 4-12. *Examples of SWIW breakthrough curves for combinations of fractures with unequal dispersivity.*

5 Discussion and conclusions

A simple radial flow and transport model with homogeneous immobile regions was employed to further evaluate a SWIW experiment in the section 422.3–423.3 m in the borehole KSH02. A few generic examples are presented along with examples of best-fit regression analysis of experimental data.

The regression analysis indicates that inclusion of diffusion-type processes may improve the fit between model and data for this test, compared with previous evaluation with an advection-dispersion model.

However, the regression fits generally required relatively high values of the parameters controlling diffusion and sorption in the matrix. Such high values are not uncommonly interpreted from tracer experiments in rock fractures and has been attributed to factors such as high-porosity fracture rim zones, fault gouge material or diffusion into larger volumes of stagnant water /Andersson and Byegård 2002/. This was also the reason for employing a model with an added rim zone.

A general impression from this study is that it may be difficult to clearly indicate that matrix diffusion, in the intact rock matrix, is a significant transport process during the particular field experiment under study. On the other hand, because of the improved ability to fit the tail of the Uranine breakthrough curve, this study indicates that diffusion-controlled processes to some extent may influence tracer transport. It may also be argued that the results indicate that such processes may be dominated by immobile zones with relatively high porosity, such as fracture rim zones and/or non-flowing parts of the fracture.

Sorption in an assumed rim zone appears to be sufficient to explain the Cs breakthrough curve, while the basic matrix diffusion model results in sorption coefficients that may be unreasonably large, although literature values for Cesium vary within a fairly wide range /Ohlsson and Neretnieks 1995/. Tailing effects of the non-sorbing tracers may be explained by some type of immobile regions or zones with relatively high porosity.

If the interpretation is correct that fracture surface sorption is dominant (in the rim zone), then previous basic evaluation (without immobile regions) may provide a fairly representative fracture retardation factor for the sorbing tracer, despite the lack of fit in the tail of the non-sorbing tracer curve.

Although the results indicate that diffusion processes may be occurring during the studied SWIW experiment, a SWIW experiment set up for detecting matrix diffusion in the intact rock may require longer experimental times, primarily using a longer waiting phase. Further, strongly sorbing tracers (such as Cs) may be less suitable for studying matrix diffusion because sorption is so dominant. It appears likely that a combination of non-sorbing tracers with significantly different diffusion coefficients, preferably in combination with longer waiting times, is the only realistic approach to clearly indicate diffusion effects. The chaser phase should then be no longer than what is needed to push the tracers a few metres or so out into the formation.

As often is the case in field tests, multiple interpretations with a number of different interpretation models may be possible. It is of practical value that interpretation models routinely applied should be as simple as possible while at the same time also be plausible. A simple model approach such as the one employed in this study appears to be plausible, because of good model fit, and may be considered as a complement to the currently routinely employed interpretation model with only advection, dispersion and equilibrium sorption as transport processes.

Generic simulations with multiple fractures with advection and dispersion only did not indicate that this would be a plausible explanation for the experimental SWIW data.

References

Andersson P, 1995. Compilation of tracer tests in fractured rock. SKB PR 25-95-05, Svensk Kärnbränslehantering AB.

Andersson P, Byegård J, 2002. Final report of the TRUE Block Scale project. 2. Tracer tests in the block scale. SKB TR-02-14, Svensk Kärnbränslehantering AB.

Becker M W, Shapiro A M, 2003. Interpreting tracer breakthrough from different forced-gradient tracer experiment configurations in fractured bedrock. Water Resources Research, vol. 39, no. 1.

Gustafsson E, Nordqvist R, 2005. Oskarshamn site investigation. Ground water flow measurements and SWIW tests in borehole KLX02 and KSH02. SKB P-05-28, Svensk Kärnbränslehantering AB.

Gustafsson E, Nordqvist R, Thur P, 2005. Forsmark site investigations. Groundwater flow measurements in boreholes KFM01A, KFM02A, KFM03A, KFM03B and SWIW tests in KFM02A, KFM03A. SKB P-05-77, Svensk Kärnbränslehantering AB.

Lessoff S C, Konikow L K, 1997. Ambiguity in measuring matrix diffusion with single-well injection/recovery tracer tests. Groundwater 35, no. 1: 166–175.

Nordqvist R, Gustafsson E, 2002. Single-well injection-withdrawal tests (SWIW). Literature review and scoping calculations for homogeneous crystalline bedrock conditions. SKB R-02-34, Svensk Kärnbränslehantering AB.

Nordqvist R, Gustafsson E, 2004. Single-well injection-withdrawal tests (SWIW). Investigation and evaluation aspects under heterogeneous crystalline bedrock conditions. SKB R-04-57, Svensk Kärnbränslehantering AB.

Ohlsson Y, Neretnieks I, 1995. Literature survey of matrix diffusion theory and of experiments and data including natural analogues. SKB TR 95-12, Svensk Kärnbränslehantering AB.

Voss C I, 1984. SUTRA – Saturated-Unsaturated Transport. A finite element simulation model for saturated-unsaturated fluid-density-dependent ground-water flow with energy transport or chemically-reactive singel-species solute transport. U.S. Geological Survey Water-Resources Investigations Report 84-4369.